An Anatomical Atlas-Based Method for Efficient Generation and Registration of 3D DOT Image Findings

Y. Xu[1,2], Y. Pei[2], R.L. Barbour[1,2]

[1]SUNY Downstate Medical Center; [2]NIRx Medical Technologies LLC

Introduction

Near-infrared optical imaging, including functional diffusion optical tomography (fDOT) and functional near-infrared spectroscopy (fNIRS), is an emerging neuroimaging technique for the noninvasive monitoring of human cerebral hemodynamics with high temporal resolution and low cost. For functional neuroimaging modalities, a capability that is increasingly regarded as essential is the ability to map image findings to the underlying anatomy. In the case of DOT imaging, complicating the goal of mapping DOT activation findings to brain anatomy is the need for a representative atlas that can support the flexible generation of the imaging operator for any selected optode arrangement. Whereas access to individual structural maps is increasingly common, efforts to generate individualized finite element method (FEM) meshes in support of DOT reconstruction can be burdensome. To facilitate the accurate generation and mapping of DOT findings, we have established a library of FEM meshes from a selected MRI atlas that has been segmented according to different tissue types. Specification of optode arrangement corresponding to individual or multiple head regions is made either by graphical selection, or through the loading of measures of head-shape and optode position followed by an affine transformation based on measured fiducials. This information is used to configure the corresponding imaging operators obtained from a precalculated database. Experimental evaluation has shown that determination of head shape, optode location, reconstruction of activation maps and mapping to individual atlases can be made with high fidelity.

Methods

MR-based FEM model library:

- Establish segmented FEM brain atlas from MRI of selected subject using EMSE software suite [1].
- Divide brain into 25 overlapping regions comprising 3000-3500 nodes with each region having a surface area of 50-75 cm^2 and a maximum depth of up to 5 cm.
- Compute solutions to forward diffusion problem using Type III boundary conditions for each of nearly 400 outer surface nodes.
- Compute joint intensity probabilities all possible source-detector combinations to generate associated Jacobian matrix (~160,000 pairs/ROI). Figure 1(B) shows twelve ROI meshes.

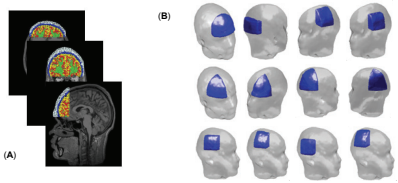

Figure 1. MRI-based segmented FEM brain mesh library.

In each ROI mesh there are about 400 boundary nodes on the surface of the head with approximately a 4 mm spatial resolution. We consider the surface nodes as the possible source/detector positions, and numerically solve the FEM discretized photon diffusion equations [2]:

$$[A]\{\Phi\} = \{b\}$$
$$[A]\{\partial\Phi/\partial\chi\} = \{\partial b/\partial\chi\} - [\partial A/\partial\chi]\{\Phi\}$$

The solutions of above equations {Φ} and {∂Φ/∂χ} are the reference detector values and wieght functions (Jacobian operators), respectively. The pre-calculated results are incorporated into the FEM model database. The complete brain FEM model database represents over 200 G bytes of data.

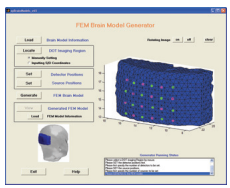

Figure 2. FEM Brain Model Generator.

To efficiently and conveniently employ the model library, we have developed a Matlab-based interactive FEM model generation tool: FEM Brain Model Generator, as shown in Figure 2. By using the generator, the users can easily generate themselves FEM brain models matching the experimental source/detector geometries by inputting the coordinates of source/detector positions and brain fiducial points measured by 3D digitizer, or by using the generator GUI to manually specify source and detector positions on the head surface of the image atlas.

3D Digitizing and registration: For accurately mapping the optode-position information from an individual subject to an FEM library model, it is necessary to first digitize brain fiducial points and source/detector positions and then to calculate the affine transformation matrix. The fiducials and optode positions can be measured by a commercial 3D digitizer, e.g., Polhemus patriot, as shown in Figure 3(A). Figure 3(B) illustrates thirteen 10-20 system points that are selected as the standard head shape fiducials in our method. The measured coordinates (P_f) of 13 fiducial points on individual subject head surface and the known coordinates (P_0) of 13 fiducial points on the image atlas surface are related by an affine transformation matrix (M) [3]:

$$P_0 = P_f M$$

where

$$P_0 = \begin{bmatrix} x_1 & y_1 & z_1 & 1 \\ x_2 & y_2 & z_2 & 1 \\ \vdots & \vdots & \vdots & \vdots \\ x_{13} & y_{13} & z_{13} & 1 \end{bmatrix}, \quad P_f = \begin{bmatrix} x_{f1} & y_{f1} & z_{f1} & 1 \\ x_{f2} & y_{f2} & z_{f2} & 1 \\ \vdots & \vdots & \vdots & \vdots \\ x_{f13} & y_{f13} & z_{f13} & 1 \end{bmatrix}, \quad M = \begin{bmatrix} m_{11} & m_{12} & m_{13} & 0 \\ m_{21} & m_{22} & m_{23} & 0 \\ m_{31} & m_{32} & m_{33} & 0 \\ m_{41} & m_{42} & m_{43} & 1 \end{bmatrix}.$$

From the equation above, the affine transformation matrix M can be sovled by least square method using matrix left division: $M = P_f \backslash P_0$

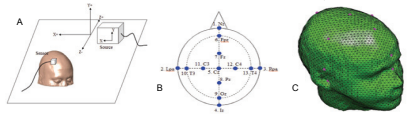

Figure 3. (A) 3D Digitizing; (B) Definition of fiducial points; (C) Image atlas and fiducial points (pink dots).

So, the measured optode coordinates P_d are registered to the image atlas by following affine transformation: $P_i = P_d M$

where P_i is the registered optode coordinate matrix.

As mentioned above, the registration of optodes to the image atlas can automatically be carried out by only loading the digitized optode and head fiducial coordinates into the FEM Brain Model Generator.

Anatomical labeling of DOT image: The considered capability has been integrated into our NAVI computing environment [4] to support model-based DOT reconstruction and generation of MR-based montages. Also available are tool boxes that support mapping of the atlas-based reconstructions to other selected atlases (individual, other). This makes it possible that our DOT images are compatible with useful public resources for anatomical analysis. As an extension of our method, we have registered the AAL (Automated Anatomical Labeling) brain atlas, in which 90 anatomical volumes of interest were reconstructed and assigned a label [5], to our image atlas by an affine transformation, as shown in Figure 4. So our registered DOT images can subsequently be queried to identify specific brain regions identified by the AAL labels. Some anatomical labeling results are shown in next section.

Figure 4. (A) Image atlas; (B) AAL brain atlas; (C) Registration of AAL brain onto image brain.

Results

Qualitative and quantitative assessments of the fidelity of our method are presented in this section. Shown in Figure 5 and Table 1 are experimental results of 3D digitizing and registration for four points on a solid brain phantom. Figure 5(A) shows the comparison of the spatial contours from the phantom (blue) and the corresponding contours from the image atlas (green). Figures 5(B) and 5(C) show the four registered points on the image atlas. Listed in the Table 1 are measures of the precision (CV = ~0.1%) and accuracy (2-5 mm error) of this registration for eight consecutive trials.

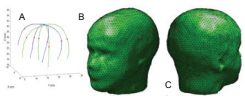

Figure 5. (A) Comparison of the spatial contours: phantom (blue) and image atlas (green); (B) and (C) Registered points on image atlas: ideal (red) and registered (pink).

Measured	P1			P2			P3			P4		
Point	1	2	3	1	2	3	1	2	3	1	2	3
Ideal	11.09	4.476	20.97	12.68	22.72	19.31	20.83	12.52	18.48	4.791	12.43	18.14
Registered	11.37	4.797	20.74	12.87	22.93	19.68	20.91	12.84	18.27	4.712	12.67	18.00
STD	0.036	0.011	0.035	0.044	0.033	0.031	0.009	0.032	0.053	0.009	0.029	0.041
Distance (I.A.R)	0.3993			0.4350			0.3028			0.2905		

Table 1. Quantitative results and accuracy of registration.

Shown in Figure 6 is an example of our method applied to simulated data (object position identified in top row). Shown in the middle row is the reconstructed image overlaid onto the Image Atlas. In the bottom row is the corresponding result registered to a subject MR map. Note that whereas the orientation and head shape of the subject is noticeably different from the Image Atlas, registration to the subject's MR is map is quite accurate.

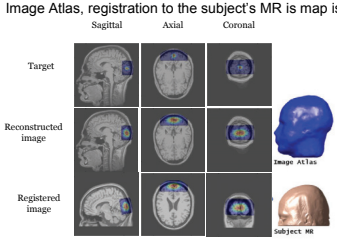

Figure 6. Reconstructed images from simulated data.

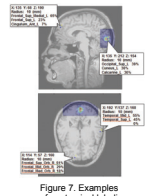

Figure 7. Examples of anatomical labeling

Results in Figure 7 are examples of anatomical labeling of overlaid DOT images. We can conveniently label our DOT images with AAL anatomical labels by clicking mouse, because we have registered the AAL brain atlas onto our image atlas.

The reconstructed DOT images from phantom experimental data are presented in Figures 8 and 9. In this experiment a solid-state programmable brain phantom [6] with a 1.2x1.2x0.2 (cm^3) liquid crystal (LC) cell, which is embeded in right frontal brain with a depth of ~2 cm below the head surface, has used to mimic the spatiotemporal hemodynamic pattern of interest. Shown in Figure 8 are reconstructed GLM log p-Value maps, where the location of LC cell is accuratly recovered. The FFTs of driven signal and reconstructed signal at cell's position are shown in Figure 9 illustrating excellent recovery of induced signal.

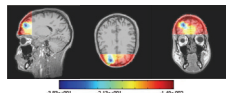

Figure 8. Reconstructed GLM log p-value images from phantom experimental data.

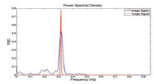

Figure 9. Power spectral density distributions of LC cell driven signal (red) and reconstructed signal (blue).

Recently, some capabilities have been extended to visualize the NIRS data. Examples are presented in Figure 10.

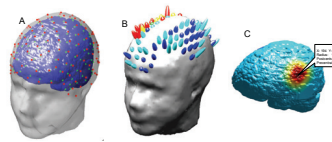

Figure 10. (A) Extended 10-20 system points registered onto the image atlas; (B) Multi-dimensional NIRS data visualization using hyperquadric glyphs; (C) Cortical map and anatomical labeling.

Conclusions

In summary, we have developed an anatomical atlas-based method for efficient generation and registration of 3D DOT image findings. As confirmed by numerical simulations and experimental data from solid-state programmable phantoms, our method is computation-efficient and is able to carry out, with high spatial and temporal accuracies, the necessary mappings—of optode-position information from an individual subject to an FEM library model, and of volumetric image information from the model back to the individual.

References

[1] http://www.sourcesignal.com

[2] K. D. Paulsen and H. Jiang, "Spatially-varying optical property reconstruction using a finite element diffusion equation approximation," *Med. Phys.*, vol. 22, pp. 691–702, 1995.

[3] A. K. Singh, M. Okamoto, et. al., "Spatial registration of multichannel multi-subject fNIRS data to MNI space without MRI," NeuroImage, 27, 842-851, 2005.

[4] Y. Pei, Y. Xu, and R.L. Barbour, "NAVI-SciPort solution: A problem solving environment (PSE) for NIRS data analysis," Poster No. 221 M-AM at Human Brain Mapping 2007 (Chicago, IL, June 10-14, 2007).

[5] N. Tzourio-Mazoyer, B. Landeau, et. al., "Automated Anatomical Labeling og Activations in SPM Using a Macroscopic Anatomical Parcellation of the MNI MRI Single-Subject Brain," NeuroImage, 15, 273-289, 2002.

[6] R.L. Barbour, R. Ansari, R. Al abdi, et. al., "Validation of near infrared spectroscopic (NIRS) imaging using programmable phantoms," *Proceedings of SPIE, Vol. 6870*, R.J. Nordstrom, Ed. (2008).

This work was supported under grant nos. 1R41NS050007-01, 1R42NS050007-02, and 2R44NS049734-02.